

DOI: 10.1002/asia.201402095

Kinetic Assay of the Michael Addition-Like Thiol–Ene Reaction and Insight into Protein Bioconjugation

Fei-He Ma, Jia-Liang Chen, Qing-Feng Li, Hui-Hui Zuo, Feng Huang, and Xun-Cheng Su*^[a]

Abstract: The chemical modification of proteins is a valuable technique in understanding the functions, interactions, and dynamics of proteins. Reactivity and selectivity are key issues in current chemical modification of proteins. The Michael addition-like thiol–ene reaction is a useful tool that can be used to tag proteins with high selectivity for the solvent-exposed thiol groups of proteins. To obtain insight into the bio-

conjugation of proteins with this method, a kinetic analysis was performed. New vinyl-substituted pyridine derivatives were designed and synthesized. The reactivity of these vinyl tags with L-cysteine was evaluated by UV

absorption and high-resolution NMR spectroscopy. The results show that protonation of pyridine plays a key role in the overall reaction rates. The kinetic parameters were assessed in protein modification. The different reactivities of these vinyl tags with solvent-exposed cysteine is valuable information in the selective labeling of proteins with multiple functional groups.

Keywords: conjugation · NMR spectroscopy · proteins · thiol chemistry · thiol–ene reaction

Introduction

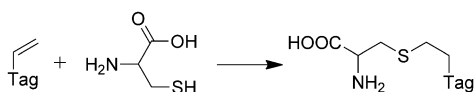
The bioconjugation of proteins with small organic probes is a powerful technique that is used in the elucidation of the structure, interaction, dynamics, and function of proteins. Small functional probes can be site-specifically attached to a protein through a chemical or biochemical method, and the optical or magnetic properties of these small molecules provide valuable information of the attached target proteins.^[1,2] In recent years, the Michael addition-like thiol–ene reaction has been used in the site-specific labeling of proteins with small molecules (Scheme 1).^[1c,3–6] The hetero-Michael thioether bond formed between the protein and the tag is resistant to reducing reagents, which avoids the down-

side of disulfide bond formation that is widely used in protein bioconjugations.

To the best of our knowledge, the Michael addition-like thiol–ene reaction was first reported in the detection of the free thiol group of proteins by use of acrylonitrile in the early 1960s.^[7] Reported examples of the formation of a hetero-Michael thioether bond as applied in protein bioconjugation can be distinguished as either radical initiated^[3,4] or a general nucleophilic addition reaction.^[5–8] The radical-initiated thiol–ene reaction plays a key role in producing functional materials and polymers in materials science.^[9] Most recently, a radical-triggered thiol–ene reaction in the modification of proteins was also reported.^[3,4]

Given the stability and activity of proteins, the thiol–ene reaction without radicals is an ideal choice for the modification of proteins. Maleimide derivatives have thus been widely used in the bioconjugation of proteins, as they readily react with the free thiol groups of proteins.^[8] However, the reaction of maleimide with the thiol group generates a new chiral center, and the formed diastereomers compromise the fluorescence, electron paramagnetic resonance (EPR), and NMR spectroscopy experimental data.^[6a] The selectivity and reactivity of the protein bioconjugation process is an important issue for some stringent assays, and mild reaction conditions are also required to maintain the structure and function of proteins. For example, high-resolution NMR spectroscopy analysis of a protein–tag conjugate is sensitive to the nonspecifically labeled protein product and the stability of the target protein, and any side tagging reaction or partial hydrolysis would result in a clear chemical shift perturbation in the high-resolution NMR spectra.

We have site-specifically labeled a protein in a chiral-free manner through a Michael addition-like thiol–ene reaction



Scheme 1. Michael addition-like thiol–ene reaction between the vinyl tag and L-cysteine.

[a] F.-H. Ma,⁺ J.-L. Chen,⁺ Q.-F. Li,⁺ H.-H. Zuo, F. Huang, Prof. X.-C. Su
State Key Laboratory of Elemento-organic Chemistry
Collaborative Innovation Center of Chemical Science and Engineering
(Tianjin)
Nankai University
Weijin Road 94, Tianjin 300071 (China)
Fax: (+86) 22-23500623
E-mail: xunchengsu@nankai.edu.cn

[⁺] These authors contributed equally to this work.

Supporting information for this article is available on the WWW under <http://dx.doi.org/10.1002/asia.201402095>.

without the assistance of radicals in aqueous solution,^[6] and the highly stable thioether between the tag and the protein offers the possibility to measure the protein complex by spectroscopic methods both in vitro and in vivo.^[6b] Chiral-free modification of proteins by using the Michael addition-like thiol–ene reaction is a simple yet promising way to tag proteins with a fluorophore or metal-ion chelator. Given that only a few examples have been reported in this field,^[6] the ligation chemistry, including the reactivity and kinetics of the reaction, needs to be elucidated in detail. To obtain insight into the bioconjugation of proteins through the formation of a thiol ether between a vinyl-substituted tag and the solvent-exposed cysteine of a protein, we designed and synthesized a number of vinyl-substituted pyridine-derived polycarboxylic acids that bind lanthanide ions strongly. The kinetic properties of these tags and L-cysteine were evaluated by means of UV absorption and high-resolution NMR spectroscopy. Protein modifications with these tags were also assessed. These kinetic parameters are valuable guidelines in the bioconjugation of proteins by using the Michael addition-like thiol–ene reaction.

Results and Discussion

Design and syntheses of the vinyl tags

The L1 (4-vinyl-DPA; DPA = dipicolinic acid) and L2 (4-vinyl-(pyridine-2,6-diyl)bismethylenitrilo tetrakis(acetic acid), 4VPMTA) tags have been shown to be site-specifically attached to a protein without radical initiation.^[6] To systematically evaluate the kinetic properties of the Michael addition-like thiol–ene reaction, L3 and L4 (Figure 1) were designed. All the tags are vinyl-substituted pyridine derivatives that contain a terminal vinyl group and a metal-ion chelating group. The synthesis of L3 and L4 is depicted in Schemes 2 and 3, respectively. 2,2':6',2''-Terpyridine-6,6''-dicarboxylic acid (TDA) is an excellent lanthanide chelator,^[10] and its homologue L3 (4-vinyl-TDA) was designed on the basis of its high rigidity and feasibility to label proteins in a site-specific manner with paramagnetic lanthanide ions.^[10b]

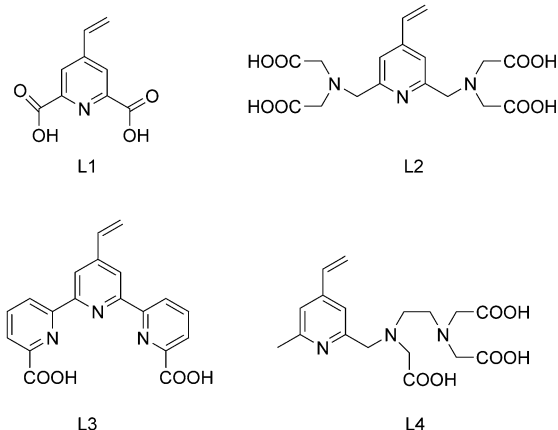
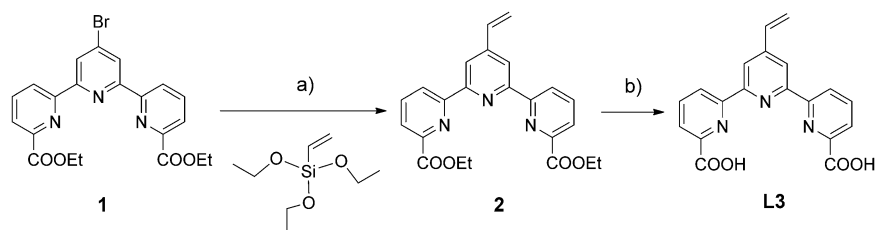
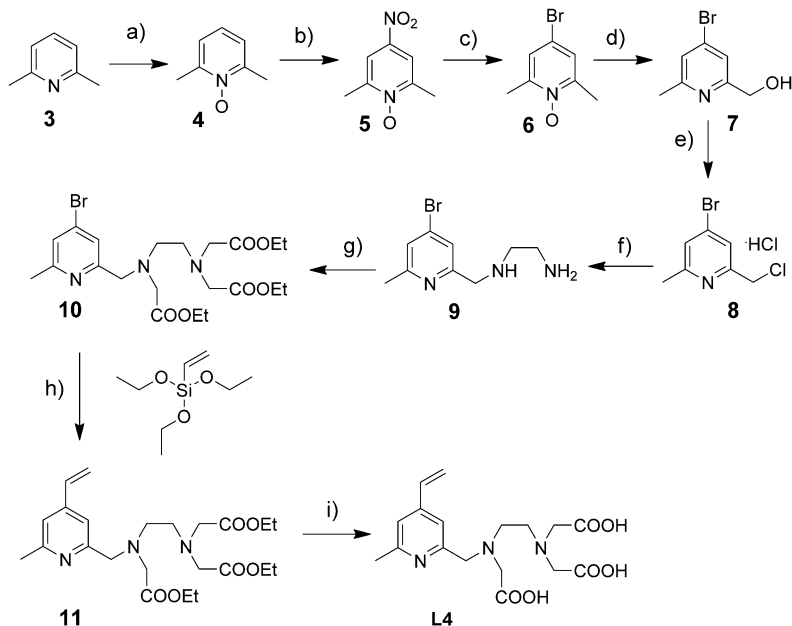


Figure 1. Structure of the vinyl tags used in protein bioconjugation.



Scheme 2. Synthesis of L3. Reagents and conditions: a) Pd(OAc)₂/TBAF/PPh₃/DMF; b) 1. NaOH/acetone, 2. HCl/H₂O. TBAF = tetrabutylammonium fluoride.



Scheme 3. Synthesis of L4. Reagents and conditions: a) AcOH, H₂O₂; b) H₂SO₄, HNO₃; c) CH₃COBr; d) (CF₃CO)₂O; e) SOCl₂; f) NH₂CH₂CH₂NH₂; g) BrCH₂COOC₂H₅, CH₃CN, DIPEA; h) Pd(OAc)₂/TBAF/PPh₃/DMF, i) 1. NaOH/H₂O, 2. HCl/H₂O. DIPEA = *N,N*-diisopropylethylamine.

Compound **1** was synthesized in four steps by using DPA as the starting material.^[11] Hiyama coupling reaction between **1** and triethoxyvinylsilane resulted in the formation of **2** in approximately 80% yield. **L3** was obtained by hydrolysis of **2** with sodium hydroxide. Starting from 2,6-dimethylpyridine (**3**), **L4** was synthesized in nine steps in a total yield of approximately 2.0%. **L4** contains a vinyl group at the 4-position in pyridine and has six atoms that can coordinate metal ions.

Kinetic assay: Chemical reaction rates and mechanism of the reaction of **L1** and **L2** with L-cysteine

To assess the reactivity of a vinyl-substituted pyridine (electron-withdrawing group) derivative towards a free thiol group in aqueous solution, we first determined the kinetic data for the reaction of **L1** with L-cysteine (Scheme 3) at pH 7.0 in 20 mM phosphate buffer at 25 °C.

The chemical reaction was monitored by observing the UV absorption change at 300 nm of **L1** with an increase in the concentration of L-cysteine (Figure 2a). In the presence of a large excess amount of L-cysteine, the second-order reaction between **L1** and L-cysteine can be written as Equations (1) and (2):

$$v = k_1^{\text{obs}}[\text{L1}] \quad (1)$$

$$k_1^{\text{obs}} = k_2^{\text{obs}}[\text{L-Cys}] \quad (2)$$

in which v is the reaction rate, k_2^{obs} is the second-order reaction rate constant, and k_1^{obs} is the pseudo-first-order reaction rate constant.

The value of k_1^{obs} , relative to a certain concentration of L-cysteine, was determined as the slope (Figure 2b) by linear fitting the UV absorption changes to the incubation time. As shown in Figure 2c, the value of k_1^{obs} increases linearly with the concentration of L-cysteine. The second-order rate constant, $k_2^{\text{obs}} = 0.03$, was determined as the slope of the linear correlation between k_1^{obs} and the concentration of L-cysteine.

To evaluate the protonation effects of pyridine on the overall reaction rates of **L1** and L-cysteine, a number of experiments were performed at different pH values in the range from 6.0 to 9.0, which would affect the protonation of pyridine. The kinetic parameters were determined. As expected, k_1^{obs} was dependent on the pH value. Notably, the observed second-order rate constant, k_2^{obs} [see Eq. (2)], increased from pH 6.0 and reached a plateau at approximately pH 7.0; it then decreased from pH 7.5 to 9.0, as shown in Figure 3 (see also Figure S1, Supporting Information). The profile of k_2^{obs} with respect to the pH value is similar to the previously reported reaction of 2-vinylpyridine with reduced glutathione,^[12] for which the maximum value of k_2^{obs} was measured at approximately pH 7.0. The striking deviations in k_2^{obs} at different pH values strongly suggest that the protonation of pyridine plays a key role in the overall reaction rate.

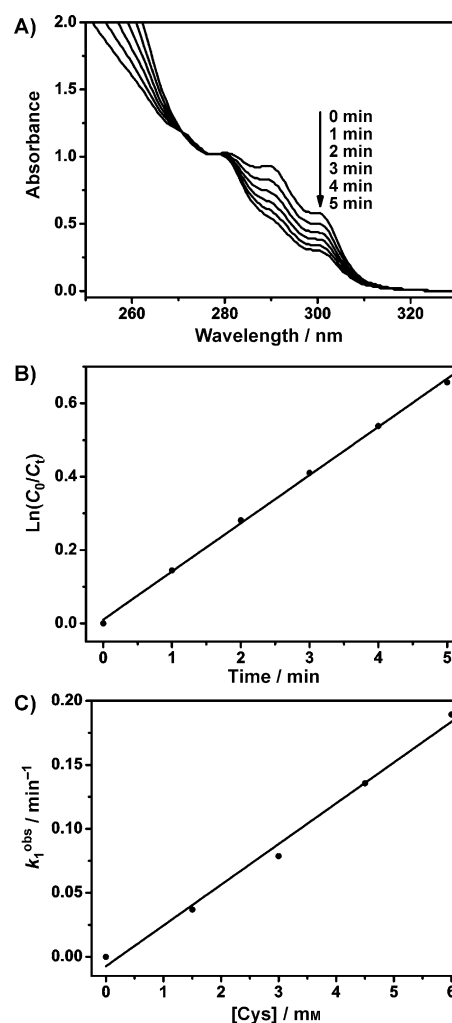


Figure 2. Kinetic evaluation of the Michael addition-like thiol-ene reaction for a mixture of **L1** and L-cysteine. a) The UV absorbance changes of **L1** in incubation with L-cysteine. 0.3 mM **L1** was incubated with 6 mM L-cysteine in 20 mM phosphate buffer at pH 7.0 and at 25 °C. b) Plot of the UV changes of **L1**, $\ln(C_0/C_t)$ at 300 nm versus the incubation time for Figure 2a, in which C_0 and C_t are the concentrations of **L1** with respect to the incubation time. The slope of the simulated curve is the pseudo-first-order rate constant, k_1^{obs} . c) Correlation of k_1^{obs} versus the concentration of L-cysteine, for which the slope gives the estimated second-order rate constant, k_2^{obs} .

It was initially assumed that the reaction between **L1** and L-cysteine first started with nucleophilic attack of deprotonated sulfhydryl, thiolate, to the terminal vinyl group of **L1**, of which the pyridine was protonated. DPA has two pK_a values, 2.2 and 6.9,^[13] and the pK_{SH} value of the thiol group of L-cysteine is approximately 8.4.^[14] Given that **L1** is similar to DPA, the pK_a of pyridine in **L1** was used as 6.9 in the data simulation. Similar to the previous analysis,^[12] the overall rates for the reaction of **L1** with L-cysteine could therefore be written as [Eq. (3)]:

$$k_2^{\text{obs}} = \frac{k^{\text{obs}}}{[\text{Cys}]} = \frac{k_2}{\left[1 + 10^{(\text{pH} - pK_a^{\text{L1}})}\right] \left[1 + 10^{(\text{p}K_{\text{SH}} - \text{pH})}\right]} \quad (3)$$

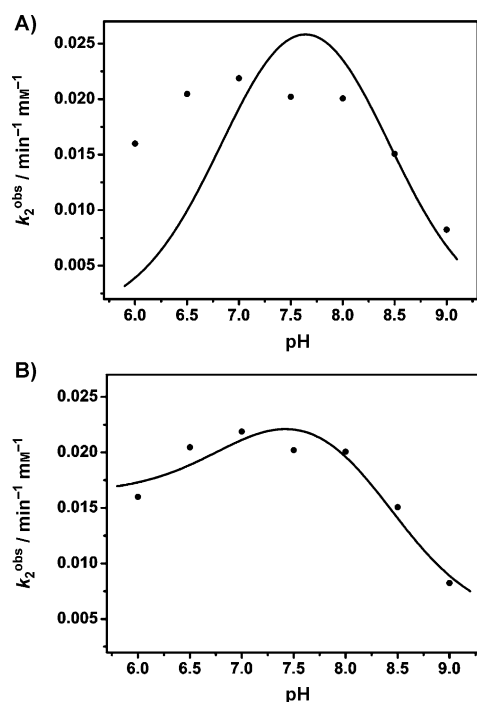


Figure 3. Plot of the experimentally determined second-order rate constant, k_2^{obs} , with respect to the corresponding pH value for the reaction of L1 with L-cysteine. The solid curve was obtained by simulation of the pH value to its determined k_2^{obs} by using a) Equation (3) and b) Equation (4). It is evident that Equation (4) gives excellent correlation between pH and k_2^{obs} .

in which k_2 is the theoretical second-order reaction rate and $\text{p}K_{\text{a}}^{\text{L1}}$ and $\text{p}K_{\text{SH}}$ are the $\text{p}K_{\text{a}}$ values of the pyridine in L1 and the sulfhydryl group of L-cysteine, respectively. However, the nonlinear fit of the experimental k_2^{obs} value to the pH values by using Equation (3) did not converge (Figure 3a), and this suggests that species in addition to those in Equation (3) also contribute to the overall reaction rates.

Taking into account these effects, we then refit the experimental data to pH values by using Equation (4), in which the chemical reaction rates of other species are included:

$$k_2^{\text{obs}} = \frac{k_1^{\text{obs}}}{[\text{Cys}]} = \left[\frac{k_1}{1 + 10^{(\text{pH} - \text{p}K_{\text{a}}^{\text{L1}})}} + \frac{k_2}{1 + 10^{(\text{p}K_{\text{a}}^{\text{L1}} - \text{pH})}} \right] \left[\frac{k_3}{1 + 10^{(\text{p}K_{\text{SH}} - \text{pH})}} + \frac{k_4}{1 + 10^{(\text{pH} - \text{p}K_{\text{SH}})}} \right] \quad (4)$$

in which $\text{p}K_{\text{a}}^{\text{L1}}$ and $\text{p}K_{\text{SH}}$ are the $\text{p}K_{\text{a}}$ values defined as in Equation (3), and k_1 , k_2 , k_3 , and k_4 are the reaction rates for each reactant species in solution.

With the known values of $\text{p}K_{\text{a}}^{\text{L1}}$ and $\text{p}K_{\text{SH}}$, the experimentally measured k_2^{obs} data were fit to the pH values by using Equation (4). Figure 3b shows excellent correlations between the experimental data and the simulated curve, and this clearly indicates the significant contributions of other species in addition to the protonated pyridine and thiolate moieties in the thiol-ene reaction. The simulated reaction

Table 1. The simulated k_1 , k_2 , k_3 , and k_4 rate constants for the reaction of L1 with L-cysteine by using Equation (4).

Reaction rate	Data
k_1	1.678
k_2	0.011
k_3	0.439
k_4	0.010

rate constants k_1 , k_2 , k_3 , and k_4 are listed in Table 1. As thiolate is a stronger nucleophile than thiol, the contributions of thiolate in the thiol-ene reaction are expected to increase with pH. Moreover, the population of protonated pyridine decreases as the pH is increased. The two controversial tendencies thus shift the overall reaction rates of the thiol-ene reaction in an opposite direction. In general, the protonated pyridine in L1 dominates the overall kinetic reaction rates in this thiol-ene addition. This is further confirmed by the estimated values of k_1 , k_2 , k_3 , and k_4 in Table 1, of which k_1 is higher than the others.

To obtain more information of the thiol-ene addition reaction for different vinyl tags, we performed similar kinetic measurements on L2 and L-cysteine. L2 was successfully used to study protein behavior in crowded media.^[6b] In addition, it forms very highly stable complexes with lanthanide metal ions.^[15] Relative to those for L1, the determined reaction rates for the mixture of L2 and L-cysteine were dramatically slower. Below pH 7.0, there was no clear reaction between L2 and L-cysteine by incubating the mixture for 5 h at room temperature. The rates for the reaction of L2 with L-cysteine increased with increasing pH. The profile of the reaction rate versus pH suggests that the content of the cysteine thiolate dominates the overall reaction rate (Figure S2), which is in great contrast to the situation with L1. The low reaction rate also indicates that the pyridine in L2 is not protonated at neutral pH, which is consistent with the determined protonation constant.^[16] Hence, to better describe the reaction mechanism, Equation (4) was rewritten as Equation (5):

$$k_2^{\text{obs}} = \frac{k_1^{\text{obs}}}{[\text{Cys}]} = \frac{k_1}{1 + 10^{(\text{p}K_{\text{SH}} - \text{pH})}} + \frac{k_2}{1 + 10^{(\text{pH} - \text{p}K_{\text{SH}})}} \quad (5)$$

In Equation (5), the term for the protonated pyridine is omitted, which results in a constant concentration for L2 in the reaction mixture. As a consequence, only the thiol and thiolate of cysteine contribute to the overall reaction rate. Figure 4 presents excellent agreement between the experimental data and the fitted curve by using Equation (5). The estimated values of k_1 and k_2 were 0.31 ± 0.03 and -0.06 ± 0.03 , respectively, which are almost identical to the values of k_3 and k_4 obtained from Equation (4) (see Table 1). The negative value of k_2 is small and negligible, which probably stems from a nonlinear fitting error. The nice-fitting curve in Figure 4 indicates that the thiolate in cysteine is the only major species in the reaction. Figures 3 and 4 both show that at a higher pH of 9.0, the determined value of k_2^{obs} in

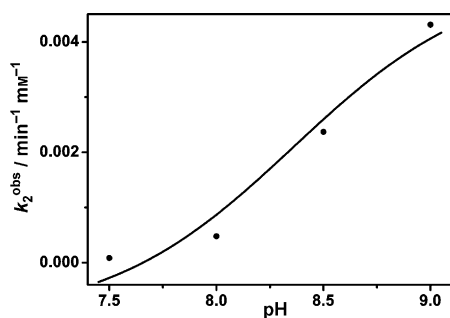


Figure 4. Kinetic assay of L2 with L-cysteine: Plot of the reaction rate constant, k_2^{obs} , with respect to pH value. The solid line was produced by nonlinear curve fitting of the pH to the experimentally determined k_2^{obs} value by using Equation (5). The value of k_2^{obs} was determined for the mixture of 0.5 mM L2 and 10 mM L-cysteine in 20 mM phosphate buffer at 25 °C.

both the L1 and L2 systems are very similar, which clearly suggests that only the reaction between the thiolate and the terminal vinyl group is present (Figure S3). The small reaction rate constants for the thiolate in cysteine and the deprotonated pyridine in both L1 and L2 suggest that an increase in the electron deficiency in the pyridine ring dramatically accelerates the overall reaction rates.

Kinetic assay of L3 and L4 with L-cysteine determined by NMR spectroscopy

In the tag of L3, the terminal vinyl-connected pyridine is substituted by two pyridine groups at the 2,6-positions. In tag L4, the 6-position is substituted by one methyl group and the 2-position is similar to the left of L2. The pK_a values of the pyridine groups in the 2,2':6',2''-terpyridine homologue were determined to be 3.55 and 4.65.^[17] At neutral pH, it can therefore be assumed that the pyridine moieties in L3 are mostly deprotonated. The reaction rate constants of L3 and L4 with L-cysteine could not be measured by UV absorption, as no significant UV absorption changes were observed by incubation of the tag with L-cysteine. Alternatively, the chemical shift of the vinyl protons for tags L3 and L4 are well resolved in the NMR spectra, and this can be used to record the reaction changes with L-cysteine. High-resolution NMR spectroscopy was then applied to monitor the signal intensities of the vinyl protons of L3 at pH 7.0 and those of L4 at pH 6.5 in 20 mM phosphate buffer and L-cysteine, respectively. The 1D ¹H NMR spectra showed that the signals for the vinyl protons gradually decreased as the incubation time with L-cysteine was increased (Figures S4 and S5). The pseudo-first-order reaction rate was determined by fitting the signal intensities of the vinyl protons to the incubation time, as shown in Figure 5. Different from L2, the reactions of L3 and L4 with L-cysteine proceeded quickly. For the mixture of L4 and cysteine, the reaction was almost complete within in 1 h.

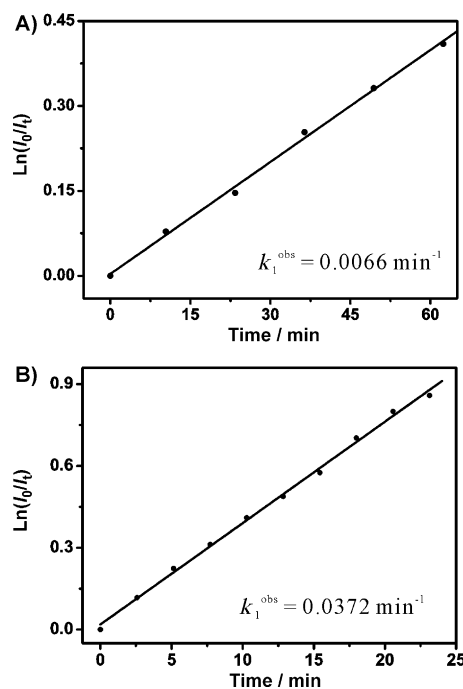


Figure 5. Kinetic assay of L3 and L4 with L-cysteine. The intensity ratio of the vinyl protons was plotted against the incubation time with L-cysteine. I_0 and I_t represent the signal intensity of the vinyl protons in the absence of L-cysteine and incubated with 6.0 mM L-cysteine at time point, respectively.

Comparison of the reaction rates of the different tags with free thiols

The four vinyl tags L1–L4 share one common structural analogue, and that is that the pyridine is substituted by a terminal vinyl group at the 4-position. However, the terminal vinyl group in these tags shows strikingly different reactivities with L-cysteine. Protonation of the pyridine group that is directly connected to the vinyl group plays a key role in the overall reaction rates of the Michael addition like thiolene reaction. L4 has lower reactivity than L1 but higher reactivity than L3 and L2. This is probably due to the partial protonation of the pyridine ring in L4 at neutral pH. L2 has the lowest reactivity of the four tags, and this is because at the measured pH value the pyridine group in L2 is deprotonated and the reaction rate only depends on the population of the deprotonated thiolate. Notably, these vinyl tags only selectively react with free thiol groups; they do not react with any of the amine groups in any of the natural amino acids.^[6b] Taken together, the reactivity order towards free thiol can be assigned as $L2 < L3 < L4 < L1$, as listed in Table 2.

Protein bioconjugation and NMR spectroscopy analysis

As the determined reactivity order of these vinyl tags towards free thiol groups can be used as a guideline for protein chemistry, we applied this concept to protein bioconjugation. L1 was successfully attached to the human ubiquitin

Table 2. The second-order rate constant, k_2^{obs} , determined for the vinyl tags.^[a]

Tag	k_2^{obs} [$\text{h}^{-1}\text{mM}^{-1}$]						
	pH 6.0	pH 6.5	pH 7.0	pH 7.5	pH 8.0	pH 8.5	pH 9.0
L1	0.960	1.228	1.314	1.213	1.205	0.904	0.495
L2	ND ^[b]	ND ^[b]	ND ^[b]	0.005	0.029	0.142	0.259
L3	–	–	0.066	–	–	–	–
L4	–	0.372	ND ^[c]	–	–	–	–

[a] The rate constants for the reactions of L1 and L2 with L-cysteine were determined by UV absorption, and those for the reactions of L3 and L4 with L-cysteine were determined by NMR spectroscopy. [b] Not detectable owing to a reaction rate that was too slow. [c] Not detectable owing to a reaction rate that was too fast.

T22C mutant by incubation of the protein with L1 for approximately 16–48 h at pH 7.6.^[6a] The reactivities of these vinyl tags with the free thiol group in the protein were assessed, and the performance for the vinyl tags in the reaction with the protein was evaluated by 2D ^{15}N - ^1H heteronuclear single quantum coherence (^{15}N HSQC) spectroscopy. To better compare the reactivity and specificity of the protein modifications with these vinyl tags, the ^{15}N -labeled human ubiquitin T22C mutant was designed, overexpressed, and purified. In the structure of ubiquitin, residue T22 resides in the beginning of the α helix and its side chain is exposed to the solvent. There is only one cysteine residue in the T22C mutant, and the reaction can be monitored by the chemical shift changes close to the ligation site, as the chemical shift is sensitive to changes in the local chemical environment. At pH 7.6 in 20 mM tris(hydroxymethyl)aminomethane (Tris) buffer, 0.1 mM ^{15}N -ubiquitin T22C was separately mixed with L1, L2, L3, and L4 (10 equiv.). After incubation, the excess amount of the vinyl tag was removed through an ion-exchange column with fast protein liquid chromatography (FPLC), and the ^{15}N HSQC spectrum was recorded for the mixture of the protein and protein-tag complex. Figure 6 presents the superimposed ^{15}N HSQC spectra of T22C before and after incubation with vinyl tags with different times. It is evident that in the ^{15}N HSQC spectrum of L1 with T22C, the cross-signals of the free protein, especially those close to the T22C residue, disappeared completely and a new set of signals appeared. This suggests that T22C was fully converted into T22C-L1. As for the mixture of T22C and L2, the two ^{15}N HSQC spectra were almost identical, which indicates that no reaction took place between the T22C mutant and L2. The notably different results between the ligation of L2 with T22C and the previously reported G47C^[6b] mutants may suggest that the microstructural environment of cysteine in the protein affects the reactivity of cysteine.

In Figure 6c,d, a new set of cross-signals was generated for separate mixtures of T22C with L3 and L4, which suggests that the thioether bond was formed between the protein and the vinyl tag. Moreover, the cross-signals of the free T22C mutant decreased in intensity. The content of the protein-tag complex was quantitatively measured by comparison of the cross-signal volumes for the free and tag-modified proteins. After incubation with the vinyl tags (10 equiv.) for 24 h, approximately 45% of the T22C protein was labeled with L3 and nearly 85% was labeled with L4.

The ligation yield is in good agreement with the reactivity assay of these vinyl tags. Taken together, we have shown that the reactivity of the vinyl tags in tagging proteins follows the order L1, L4, L3, and L2. Notably, the cysteine in different secondary structures of a protein displays varied reactivity towards the vinyl tags, as shown in L2.

We then further explored the reactivity of cysteine in different secondary structures of a protein. Two single-point ubiquitin mutants A28C and E64C were made, and the ^{15}N -labeled protein samples were expressed and purified. In the structure of ubiquitin, T22 resides in the beginning of the first α helix, A28 resides in the first α helix, and E64 resides in the long loop region after the fifth β sheet. Under the same conditions as those used in Figure 6a, the A28C and E64C mutants showed greatly differing reactivities in the reaction with L3. The E64C mutant was fully converted into E64C-L3, whereas no clear reaction was observed for A28C, as shown in Figure 6d,e. In summary, it is plausible that a residue in a well-structured region shows lower activity than that in a flexible loop or unstructured segment.

Conclusions

The Michael addition-like thiol-ene reaction is a promising way to label proteins in a site-specific way with fluorophore or metal-chelating tags in a chiral-free and highly stable manner. The rate of the reaction between the vinyl tags and the thiol group of the cysteine residue is an important issue that was addressed in the present study, as it determines the ligation yield of the proteins. Without radical assistance, the reaction between the vinyl-substituted pyridine derivatives and cysteine proceeded in aqueous solution at different reaction rates. Protonation of the vinyl-substituted pyridine enhanced the thiol-ene reaction greatly at neutral pH. For the vinyl tags substituted with unprotonated pyridine, a higher pH was required to fulfill the reaction. Conceivably, the reactivity assay of these vinyl tags with L-cysteine was applied in protein bioconjugation. In addition, we showed that the cysteine residue in different secondary structures of a protein shows strikingly different reactivity towards the vinyl tags. Together, we showed that these novel vinyl tags allow differentiation of the reactivity of different cysteine residues in a protein, which makes it possible to label proteins with multiple tags at different sites. The kinetic parameters determined in this study will serve as a valuable guideline in vinyl-substituted pyridine derivatives for protein modification.

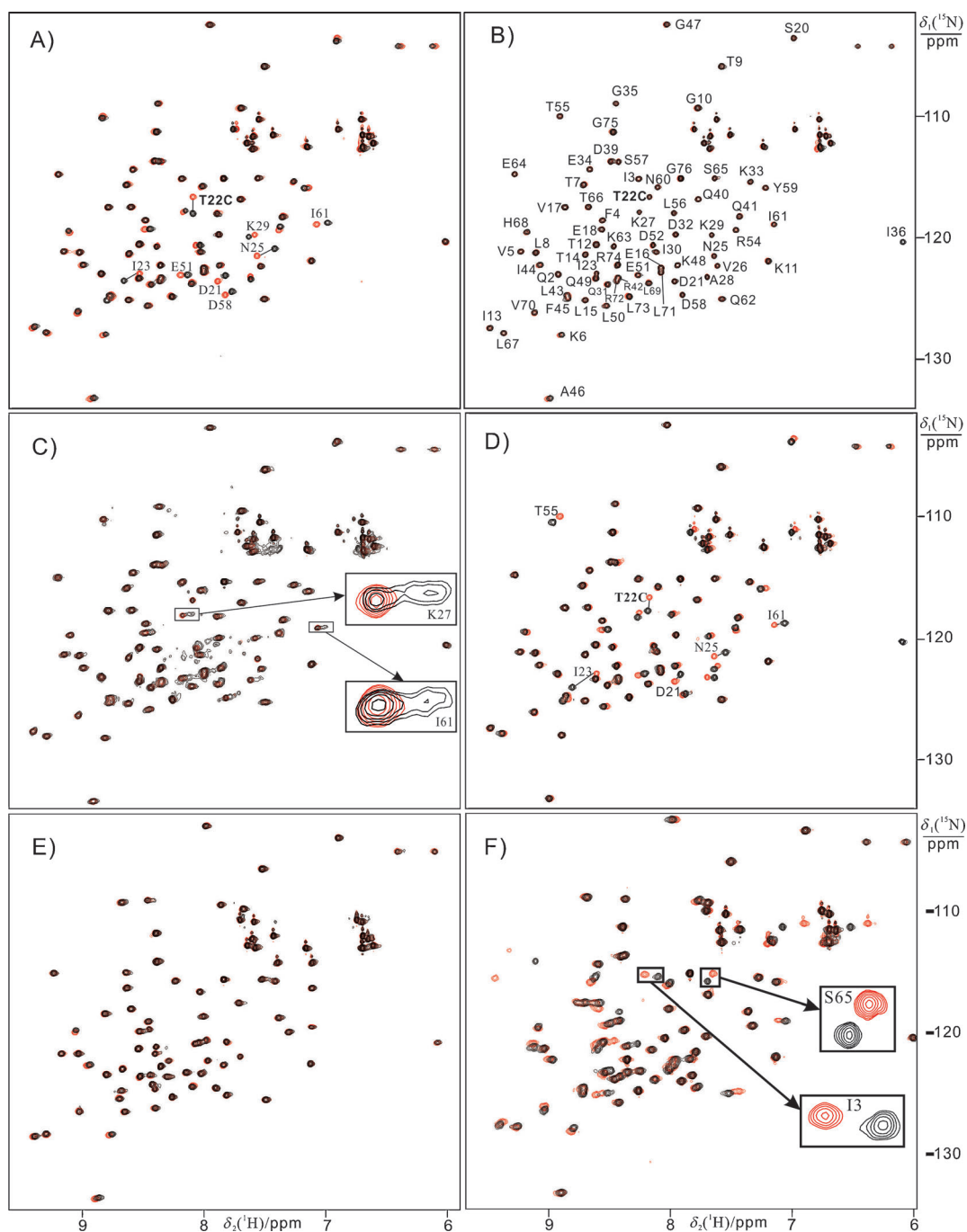


Figure 6. Superimposition of the ^{15}N HSQC spectra of 0.1 mM uniformly ^{15}N -labeled ubiquitin mutant incubated in the absence (red) and presence of 1.0 mM vinyl tag (black), and then the excess amount of the tags was removed by FPLC (fractions of the protein-tag complex and the free protein were combined for NMR spectroscopy measurements) and the pH was adjusted to 6.4. a) T22C-L1 incubated at pH 7.6 in 20 mM Tris at 25 °C for 24 h; b) T22C-L2 incubated at pH 8.0 in 20 mM Tris at 30 °C for 2.5 days; c) T22C-L3 under the same conditions as those given in a); d) T22C-L4 incubated at pH 7.6 in 20 mM Tris at 25 °C for 1.5 days, and the protein was fully converted into T22C-L4; e) A28C-L3 under the same conditions as those given in a); f) E64C-L3 under the same conditions as those given in a).

Experimental Section

Syntheses

1: Synthesized from dipicolinic acid, as previously reported.^[11]

2: Compound **1** (0.114 g, 0.25 mmol), Pd(OAc)₂ (5.61 mg, 0.025 mmol), and PPh₃ (13.10 mg, 0.05 mmol) were dissolved in DMF (5 mL), and then triethoxyvinylsilane (0.10 mL, 0.50 mmol) and tetrabutylammonium bro-

midate (TBAB; 0.5 mL, 0.50 mmol) in THF stock were added stepwise to the above mixture under an atmosphere of argon. The resulting solution was stirred at 85 °C for 12 h and then cooled down to room temperature. Water (5 mL) was added to the solution, and the mixture was extracted with ethyl acetate (2 × 10 mL). The combined organic phase was washed with brine, dried with anhydrous sodium sulfate, filtered, and then concentrated under reduced pressure. The resulting yellowish oil was puri-

fied by chromatography [silica gel; petroleum ether (b.p. 60–90°C)/ethyl acetate=3:1]. A white solid (0.086 g, ≈80%) was obtained. ¹H NMR (400 MHz, CDCl₃): δ=8.88–8.76 (m, 2H), 8.70–8.62 (m, 2H), 8.19 (dd, *J*=10.9, 4.2 Hz, 2H), 8.04 (dd, *J*=7.8, 4.4 Hz, 2H), 6.96 (dd, *J*=17.6, 10.9 Hz, 1H), 6.29 (d, *J*=17.6 Hz, 1H), 5.64 (d, *J*=10.9 Hz, 1H), 4.55 (q, *J*=7.13 Hz, 4H), 1.52 ppm (t, *J*=7.32 Hz, 6H). ¹³C NMR (101 MHz, CDCl₃): δ=165.35, 156.35, 154.97, 147.85, 147.14, 137.80, 135.01, 125.08, 124.37, 119.40, 119.20, 61.96, 14.36 ppm.

L3. Compound **2** (0.46 g, 1.14 mmol) was dissolved in acetone (20 mL) and 2 M NaOH (10 mL, 22 mmol) in water solution was added. The mixture was then stirred for approximately 2 h. 6 M HCl was added to neutralize the above mixture until no more white precipitate was formed. The precipitate was filtered and dried. The yield was approximately 73%. ¹H NMR (600 MHz, D₂O): δ=5.53 (d, *J*=11.3 Hz, 1H), 6.23 (d, *J*=16.5 Hz, 1H), 6.82 (dd, *J*=16.5, 11.3 Hz, 2H), 7.85 (d, *J*=7.85 Hz, 2H), 7.95 (t, *J*=7.85 Hz, 2H), 8.27 (m, 2H), 8.32 ppm (s, 2H).

4 and 5: Synthesized as previously reported.^[18]

6: Similar to a previous report,^[19] acetyl bromide (35 mL, 470 mmol) was added dropwise to a solution of **5** (2.5 g, 148 mmol) in glacial AcOH (35 mL) at 55°C. The resulting mixture was stirred for approximately 5 h. After cooling to room temperature, water (200 mL) was added to the solution, and the pH was adjusted to pH 10 with K₂CO₃ powder. The above mixture was extracted with ethyl acetate (2×). The organic phase was dried with Na₂SO₄, and the solvent was removed under reduced pressure, which resulted in a yellow powder (75%). ¹H NMR (400 MHz, CDCl₃): δ=8.04 (s, 2H), 2.59 ppm (s, 6H).

7: Trifluoroacetic anhydride (8 mL, 53 mmol) was added dropwise to a solution of **6** (2.0 g, 9 mmol) in dry CH₂Cl₂ (25 mL) at 0°C. The resulting solution was heated at reflux for approximately 15 h with stirring. After cooling to room temperature, the solvent was removed under reduced pressure. The resulting powder was mixed with a saturated aqueous solution of K₂CO₃ (10 mL), and the mixture was stirred for 2 h. The above mixture was extracted with ethyl acetate, and the organic phase was dried with Na₂SO₄. The solvent was removed under reduced pressure, which resulted in a yellow solid (1.30 g, 65%). ¹H NMR (400 MHz, CDCl₃): δ=7.32 (s, 1H), 7.30 (s, 1H), 4.74 (s, 2H), 2.58 ppm (s, 3H).

8: SOCl₂ (0.6 mL, 8 mmol) was added dropwise to a solution of **7** (1.0 g, 5 mmol) in dry CH₂Cl₂ (10 mL) at 0°C. The mixture was heated at reflux for 3 h. After cooling to room temperature, the solvent was removed, which resulted in a yellow solid (1.10 g, 87%). ¹H NMR (400 MHz, CDCl₃): δ=7.36 (s, 1H), 7.18 (s, 1H), 3.81 (s, 2H), 2.53 ppm (s, 3H).

9: Compound **8** (4.0 g, 15 mmol) in dry CH₃CN (30 mL) was added dropwise to ethanediamine (14 mL, 210 mmol) with stirring at room temperature, and the resulting mixture was stirred for 20 h. The produced solid was filtered off. The filtrate was removed under reduced pressure, and the remaining solid was dissolved in ethyl acetate and washed with aqueous K₂CO₃. The organic phase was dried with Na₂SO₄ and then concentrated under reduced pressure, which resulted in a yellowish oil (2.9 g, 75%). ¹H NMR (400 MHz, CDCl₃): δ=7.56 (brs, 2H), 3.91 (s, 2H), 2.85 (t, 2H), 2.73 (t, 2H), 2.55 ppm (s, 3H).

10: Ethyl bromoacetate (5.5 mL, 50 mmol) in dry CH₃CN (20 mL) was added dropwise to a solution of **9** (2.5 g, 10 mmol) in dry CH₃CN (40 mL) and DIPEA (9 mL, 50 mmol). The resulting mixture was heated to 60°C for 10 h with stirring. After cooling to room temperature, the reaction mixture was filtered. The solvent was removed under reduced pressure, and the final product was purified by chromatography [silica gel; petroleum ether (b.p. 60–90°C)/ethyl acetate=3:1] to give a yellow oil (2.7 g, 52%). ¹H NMR (400 MHz, CDCl₃): δ=7.56 (s, 1H), 7.21 (s, 1H), 4.19 (m, 6H), 3.95 (s, 2H), 3.57 (s, 4H), 3.53 (s, 2H), 2.89 (m, 4H), 2.50 (s, 3H), 1.27 ppm (m, 9H).

11: Compound **10** (0.8 g, 1 mmol), dry DMF (25 mL), triethoxyvinylsilane (0.75 mL, 1.5 mmol), and 1 M TBAF (6.5 mL, 2 mmol) in THF stock were mixed. Under an atmosphere of argon, Pd(OAc)₂ (22 mg, 0.1 mmol) and PPh₃ (85 mg, 0.3 mmol) were added. The resulting mixture was heated to 90°C with stirring for 3 h. The reactant mixture was poured into water (120 mL) and then extracted with ethyl acetate. The organic phase was washed with saturated NaCl and dried with Na₂SO₄. The organic solvent

was removed, and the final product was purified by chromatography [silica gel; petroleum ether (b.p. 60–90°C)/ethyl acetate=4:1] to give a yellowish oil (0.41 g). ¹H NMR (400 MHz, CDCl₃): δ=7.40 (s, 1H), 7.02 (s, 1H), 6.65 (dd, *J*=10.96, 17.76 Hz, 1H), 5.99 (d, *J*=17.76, 1H), 5.46 (d, *J*=10.96 Hz, 1H), 4.14 (m, 6H), 3.94 (s, 2H), 3.58 (s, 4H), 3.47 (s, 2H), 2.89 (m, 4H), 2.53 ppm (m, 9H).

L4: NaOH (0.23 g, 6 mmol) in water (2 mL) was added to a solution of **11** (0.6 g, 1 mmol) in a mixture of ethanol (5 mL) and H₂O (5 mL). The resulting solution was stirred at room temperature for 6 h. Dowex H⁺ ion-exchange resin (10.0 g) was added to the above mixture, and the solution was filtered after the pH of the suspension decreased to 3. The solvent was removed under reduced pressure, and the powder was suspended in acetone (10 mL) and filtered to yield a white solid (0.36 g, 75%). ¹H NMR (400 MHz, D₂O): δ=7.20 (s, 1H), 7.11 (s, 1H), 6.61 (dd, *J*=19.04, 11.64 Hz, 1H), 5.96 (d, *J*=19.04 Hz, 1H), 5.42 (d, *J*=11.64 Hz, 1H), 3.56 (s, 2H), 3.02 (s, 2H), 2.81(s, 4H), 2.47(m, 4H), 2.32 ppm (s, 3H).

Kinetic measurements of L1 and L2 with L-cysteine

A Shimadzu UV-2550 spectrometer was used to measure the reaction rate of the vinyl tags with L-cysteine. The reactivity of L1 was probed by recording the decrease in the UV absorption of L1 at 300 nm by incubating 0.30 mM L1 with different concentrations of L-cysteine in 20 mM phosphate-buffered saline (PBS) at different pH values at 25°C. The pseudo-first-order reaction rate, *k*₁^{obs}, was obtained by linear fit of the UV absorption changes to the incubation time. In the case of L2, the UV absorption change was monitored at 290 nm.

Protein expression and purification

The ¹⁵N-labeled ubiquitin T22C mutant was designed, expressed, and purified according to a previously published protocol.^[6a]

Protein modification with vinyl tags

A tenfold excess amount of the vinyl tag in a 50 mM aqueous solution was added to the 0.30 mM ¹⁵N-labeled protein in 2.0 mL 20 mM Tris and 0.30 mM tris(2-carboxyethyl)phosphine (TCEP) at pH 7.6. The pH of the protein solution was then adjusted to 7.6. The mixture was incubated at room temperature for 24 h. The excess amount of the free vinyl tag was removed by FPLC with an anion-exchange column, and the buffer was exchanged to 20 mM 2-(*N*-morpholino)ethanesulfonic acid (MES) at pH 6.4 for the NMR spectroscopy measurements.

NMR spectroscopy

All NMR spectra were recorded with a Bruker 600 MHz spectrometer equipped with a QCI-cryoprobe at 298 K. The kinetic studies of tags L3 and L4 with L-cysteine were evaluated by 1D NMR spectroscopy. The 1D ¹H NMR spectra were first recorded for the 1 mM vinyl tags. 100 mM L-cysteine (0.03 mL, equaled 6 mM in NMR tube) was then added to a solution of 1 mM vinyl tag in 20 mM phosphate (0.55 mL) at pH 7.0 (for L3) or 6.5 (for L4). The 1D ¹H NMR spectra were then recorded with the incubation time at 298 K. The reaction rates of L4 and L-cysteine were not determined at pH 7.0, because the reaction rates were too fast to record the NMR spectrum. The signal intensity changes of the vinyl protons in the vinyl tags were fitted to the incubation time with L-cysteine.

All 2D ¹⁵N HSQC spectra were performed at 298 K in 20 mM MES buffer (pH 6.4) for 0.1 mM protein solution. The NMR spectra were processed with Topspin 2.1 and analyzed with Sparky.^[20]

Acknowledgements

Financial support through the 973 Program (2013CB910200) and from the National Science Foundation of China (21073101, 21273121, and 21121002) is greatly acknowledged.

- [1] a) N. Stephanopoulos, M. B. Francis, *Nat. Chem. Biol.* **2011**, *7*, 876–884; b) E. M. Sletten, C. R. Bertozzi, *Angew. Chem.* **2009**, *121*, 7108–7133; *Angew. Chem. Int. Ed.* **2009**, *48*, 6974–6998; c) A. Dondoni, A. Marra, *Chem. Soc. Rev.* **2012**, *41*, 573–586; d) J. M. Chalker, G. J. Bernardes, B. G. Davis, *Acc. Chem. Res.* **2011**, *44*, 730–741; e) E. Weerapana, G. M. Simon, B. F. Cravatt, *Nat. Chem. Biol.* **2008**, *4*, 405–407; f) Y. X. Chen, G. Triola, H. Waldmann, *Acc. Chem. Res.* **2011**, *44*, 762–773; g) Y. Takaoka, A. Ojida, I. Hamachi, *Angew. Chem. Int. Ed.* **2013**, *52*, 4088–4106; *Angew. Chem.* **2013**, *125*, 4182–4200; h) C. P. Hackenberger, D. Schwarzer, *Angew. Chem. Int. Ed.* **2008**, *47*, 10030–10074; *Angew. Chem.* **2008**, *120*, 10182–10228.
- [2] a) C. H. Kim, J. Y. Axup, P. G. Schultz, *Curr. Opin. Chem. Biol.* **2013**, *17*, 412–429; b) X. C. Su, G. Otting, *J. Biomol. NMR* **2010**, *46*, 101–112; c) K. N. Allen, B. Imperiali, *Curr. Opin. Chem. Biol.* **2010**, *14*, 247–254.
- [3] a) D. Weinrich, P. C. Lin, P. Jonkheijm, U. T. T. Nguyen, H. Schroeder, C. M. Niemeyer, K. Alexandrov, R. Goody, H. Waldmann, *Angew. Chem. Int. Ed.* **2010**, *49*, 1252–1257; *Angew. Chem.* **2010**, *122*, 1274–1279; b) P. Jonkheijm, D. Weinrich, M. Koehn, H. Engelkamp, P. C. M. Christianen, J. Kuhlmann, J. C. Maan, D. Nuesse, H. Schroeder, R. Wacker, R. Breinbauer, C. M. Niemeyer, H. Waldmann, *Angew. Chem. Int. Ed.* **2008**, *47*, 4421–4424; *Angew. Chem.* **2008**, *120*, 4493–4496; c) S. Wittrock, T. Becker, H. Kunz, *Angew. Chem. Int. Ed.* **2007**, *46*, 5226–5230; *Angew. Chem.* **2007**, *119*, 5319–5323.
- [4] a) A. Dondoni, A. Massi, P. Nanni, A. Roda, *Chem. Eur. J.* **2009**, *15*, 11444–11449; b) M. Lo Conte, S. Staderini, A. Marra, M. Sanchez-Navarro, B. G. Davis, A. Dondoni, *Chem. Commun.* **2011**, *47*, 11086–11088; c) Y. Li, M. Yang, Y. Huang, X. Song, L. Liu, P. R. Chen, *Chem. Sci.* **2012**, *3*, 2766–2770; d) Y. A. Lin, J. M. Chalker, N. Floyd, G. J. Bernardes, B. G. Davis, *J. Am. Chem. Soc.* **2008**, *130*, 9642–9645; e) J. M. Chalker, Y. A. Lin, O. Boutoureira, B. G. Davis, *Chem. Commun.* **2009**, 3714–3716; f) N. Floyd, B. Vijaykrishnan, J. R. Koeppe, B. G. Davis, *Angew. Chem. Int. Ed.* **2009**, *48*, 7798–7802; *Angew. Chem.* **2009**, *121*, 7938–7942; g) J. M. Chalker, L. Lercher, N. R. Rose, C. J. Schofield, B. G. Davis, *Angew. Chem. Int. Ed.* **2012**, *51*, 1835–1839; *Angew. Chem.* **2012**, *124*, 1871–1875; h) F. Li, A. Allahverdi, R. Yang, G. B. Lua, X. Zhang, Y. Cao, N. Korolev, L. Nordenskiöld, C. F. Liu, *Angew. Chem. Int. Ed.* **2011**, *50*, 9611–9614; *Angew. Chem.* **2011**, *123*, 9785–9788; i) L. Markey, S. Giordani, E. M. Scanlan, *J. Org. Chem.* **2013**, *78*, 4270–4277.
- [5] a) J. E. T. Corrie, *J. Chem. Soc. Perkin Trans. 1* **1994**, 2975–2982; b) V. Hong, A. A. Kislukhin, M. G. Finn, *J. Am. Chem. Soc.* **2009**, *131*, 9986–9994.
- [6] a) Q. F. Li, Y. Yang, A. Maleckis, G. Otting, X. C. Su, *Chem. Commun.* **2012**, *48*, 2704–2706; b) Y. Yang, Q. F. Li, C. Cao, F. Huang, X. C. Su, *Chem. Eur. J.* **2013**, *19*, 1097–1103.
- [7] a) L. Weil, T. S. Seibles, *Arch. Biochem. Biophys.* **1961**, *95*, 470–473; b) M. Friedman, J. G. Cavins, J. S. Wall, *J. Am. Chem. Soc.* **1965**, *87*, 3672–3682.
- [8] G. T. Hermanson, *Bioconjugate Techniques*, 2nd ed., Academic Press, Amsterdam, **2008**.
- [9] a) C. E. Hoyle, A. B. Lowe, C. N. Bowman, *Chem. Soc. Rev.* **2010**, *39*, 1355–1387; b) A. Dondoni, *Angew. Chem. Int. Ed.* **2008**, *47*, 8995–8997; *Angew. Chem.* **2008**, *120*, 9133–9135; c) M. van Dijk, D. T. Rijkers, R. M. Liskamp, C. F. van Nostrum, W. E. Hennink, *Bioconjugate Chem.* **2009**, *20*, 2001–2016; d) A. Massi, D. Nanni, *Org. Biomol. Chem.* **2012**, *10*, 3791–3807.
- [10] a) E. S. Andreiadis, R. Demadrille, D. Imbert, J. Pecauc, M. Mazzanti, *Chem. Eur. J.* **2009**, *15*, 9458–9476; b) F. Huang, Y. Y. Pei, H. H. Zuo, J. L. Chen, Y. Yang, X. C. Su, *Chem. Eur. J.* **2013**, *19*, 17141–17149.
- [11] P. Kadjané, C. Plates-Iglesias, R. Ziessel, L. J. Charbonniere, *J. Chem. Soc. Dalton Trans.* **2009**, 5688–5700.
- [12] K. Lindorff-Larsen, J. R. Winther, *Anal. Biochem.* **2000**, *286*, 308–310.
- [13] J. G. Speight, *Lange's Handbook of Chemistry*, 16th ed., McGraw-Hill, New York, **2005**.
- [14] R. M. C. Dawson, D. C. Elliott, W. H. Elliott, K. M. Jones, *Data for Biochemical Research*, 3rd ed., Clarendon Press, Oxford, **1986**.
- [15] L. Pellegatti, J. Zhang, B. Drahoš, S. Villette, F. Suzenet, G. Guillaumet, S. Petoud, E. Tóth, *Chem. Commun.* **2008**, 6591–6593.
- [16] C. S. Bonnet, F. Buron, F. Caillé, C. M. Shade, B. Drahoš, L. Pellegatti, J. Zhang, S. Villette, L. Helm, C. Pichon, F. Suzenet, S. Petoud, E. Tóth, *Chem. Eur. J.* **2012**, *18*, 1419–1431.
- [17] M. K. Nazeeruddin, S. M. Zakeeruddin, R. Humphry-Baker, T. A. Kaden, M. Grätzel, *Inorg. Chem.* **2000**, *39*, 4542–4547.
- [18] A. M. Achmatowicz, L. S. Hegedus, S. David, *J. Org. Chem.* **2003**, *68*, 7661–7666.
- [19] R. C. Jones, A. J. Canty, J. A. Deverell, M. G. Gardiner, R. M. Guijt, R. Rodemann, J. A. Smith, V. A. Tolhurst, *Tetrahedron* **2009**, *65*, 7474–7481.
- [20] T. D. Goddard, D. G. Kneller, *Sparky 3*, University of California, San Francisco, **2002**.

Received: February 21, 2014

Published online: May 21, 2014